

## Regional patterns of physiological condition determine giant kelp net primary production dynamics

Tom W. Bell <sup>1\*</sup>, Daniel C. Reed,<sup>2</sup> Norman B. Nelson,<sup>1</sup> David A. Siegel<sup>1,3</sup>

<sup>1</sup>Earth Research Institute, University of California, Santa Barbara, Santa Barbara, California

<sup>2</sup>Marine Science Institute, University of California, Santa Barbara, Santa Barbara, California

<sup>3</sup>Department of Geography, University of California, Santa Barbara, Santa Barbara, California

### Abstract

Photoautotrophs vary the concentration of photosynthetic pigments in response to changing environmental conditions. In the ocean, the chlorophyll *a* to carbon ratio (Chl:C) has been used as a proxy for the physiological condition of phytoplankton, and there is laboratory evidence that the growth rate of juvenile giant kelp (*Macrocystis pyrifera*), a coastal foundation species, is positively related to Chl:C under nutrient-limited conditions. We examined the relative roles of nutrients and light in determining Chl:C dynamics and if fluctuations in Chl:C were related to changes in canopy biomass and net primary production (NPP) from sites spanning 750 km of the California coast. Seventy percent of the variability in canopy Chl:C was explained by a combination of photosynthetically active radiation and seawater nitrate concentration. In the periodically nutrient-limited waters of the Southern California Bight, changes in Chl:C positively resembled changes in available nitrate, whereas Chl:C negatively tracked changes in light for the more nutrient-replete central California coastline. Values of Chl:C were positively related to residuals from an autoregressive model of kelp biomass at the southern California sites indicating that Chl:C is a proxy for physiological state of the kelp canopy. NPP estimated through correlations with kelp biomass and lagged Chl:C compared well to established field-based estimates. These results open the possibility of assessing giant kelp physiological condition from estimates of Chl:C modeled from sea surface irradiance and nitrate concentration, which in turn can be used to estimate giant kelp primary production over large spatial and temporal scales using future remote sensing technologies.

The physiological condition of marine flora fluctuates through time and space in response to environmental variations (Behrenfeld et al. 2005). Marine autotrophs adjust to photosynthetic demands by varying cellular pigment levels in response to changes in light, nutrients, and temperature (Kirk 1994). For example, in steady state, nutrient-limited conditions, the marine diatom, *Thalassiosira weissflogii* (formerly *Thalassiosira fluviatilis*) was shown to linearly increase its cellular concentrations of chlorophyll *a* (Chl) in relation to its carbon content (Chl:C) as nutrient concentrations increased (Laws and Bannister 1980). Under nutrient-replete conditions, this species decreased its Chl:C in a nonlinear fashion in response to increased light levels. These results illustrate how fluctuations in photosynthetic machinery in response to changes in the environment are context specific.

Values of the Chl:C ratio also scale with growth rate in marine autotrophs (e.g., Shivji 1984; Geider 1987). Sakshaug et al. (1989) found that, in a nutrient-limited system, the Chl:C ratio of the marine diatom *Skeletonema costatum* was linearly proportional to its growth rate for a given level of daily irradiance. Over the past decade, results from these and other laboratory studies have been combined with large spatial scale measurements of Chl concentrations, phytoplankton carbon biomass, and incident light from satellite sensors to estimate phytoplankton growth rates for the world's oceans (Behrenfeld et al. 2005). These results suggest that macrophyte growth rates combined with biomass determinations can be used to estimate regional kelp forest net primary production (NPP).

The marine macroalga *Macrocystis pyrifera*, hereafter referred to as giant kelp, is a globally distributed, surface canopy forming species that serves as the foundation to an ecologically diverse and economically important ecosystem (Leet et al. 2001; Graham et al. 2007; Schiel and Foster 2015). Giant kelp's initial life stage is microscopic when it

\*Correspondence: [tbell@eri.ucsb.edu](mailto:tbell@eri.ucsb.edu)

Additional Supporting Information may be found in the online version of this article.

first attaches to shallow (< 30 m depth) rocky reefs, but can reach the surface and form a dense canopy within several months (Dayton et al. 1992; Reed et al. 2006). The adult plant consists of a holdfast supporting a bundle of fronds with leaf-like blades extending at regular intervals, each with a gas-filled pneumatocyst to buoy the fronds to the sea surface, where most of its biomass resides (Reed et al. 2015). The fronds commonly grow about 14–18 cm a day, which requires high concentrations of nutrients from the surrounding waters (Gerard 1982; Zimmerman and Kremer 1986; Stewart et al. 2009). Frond elongation rate increases in a nonlinear, saturating fashion in response to increased ambient nitrate concentrations (Zimmerman and Kremer 1984). Photosynthetic pigment concentrations and Chl:C are also known to increase with elevated ambient nitrate conditions and be positively associated with increases in specific growth rate under nutrient-limited laboratory conditions (Shivji 1984, 1985; Kopcak 1994; Stephens and Hepburn 2016). While changes in ambient nutrient concentrations have been implicated in changes in growth rate and physiological condition, the loss of fronds due to age-dependent, programmed senescence (roughly 100 d after frond initiation) plays a large role in kelp forest biomass dynamics (Rodriguez et al. 2013).

Rates of photosynthesis and concentrations of photosynthetic pigments vary in giant kelp in response to changes in light along a depth gradient. Pigment content of a frond increases to a maximum in the surface canopy about 2 m back from the growing tip and remains generally constant throughout much of the water column, until decreasing again in the oldest, deepest blades (Wheeler 1980; Rodriguez et al. 2016). Surface canopy blades also have higher ultraviolet absorbing compounds and photoprotective pigment concentrations than blades at depth, protecting and regulating photosynthesis in this high light environment and allowing the canopy to make the largest contribution to production (Colombo-Pallotta et al. 2006). Furthermore, while the accessory photosynthetic pigment fucoxanthin (FX) functions as a light-harvesting pigment, it can also protect against the photooxidation of cell material in high-light environments (Clayton 1980; Di Valentin et al. 2012).

While much is known about how giant kelp condition responds to changes in light over a depth gradient at a single point in time, there is a dearth of information on how canopy physiological condition changes through time or over a latitudinal gradient, and how such changes influence biomass and production dynamics. Understanding the relationships between the environment and growth of this foundation species could enable broader scale estimates of its production and its contribution to coastal food webs and community structure using remote sensing technologies. In this study, we assessed how the concentration of photosynthetic pigments and Chl:C in giant kelp varies in response to environmental variables over multiple years at sites spanning

~ 750 km of coastline in California, U.S.A. We also examined relationships between Chl:C and remotely sensed measurements of kelp canopy biomass as well as *in situ* determinations of standing foliar biomass (SFB) and NPP. We aimed to answer two overarching questions: (1) What are the relative roles of nutrients and light in determining the photosynthetic pigment and Chl:C dynamics of the giant kelp canopy? (2) Are these fluctuations in physiological condition related to changes in giant kelp biomass and NPP over ecologically relevant time scales?

## Methods

### Giant kelp condition, biomass, and NPP data

We assessed the physiological condition and biomass of the giant kelp canopy across the species' range of dominance in California, U.S.A. This region is subject to seasonal fluctuations in both the surface nutrient and light environment. Sea surface nitrate concentrations follow seasonal and geographic patterns consistent with coastal upwelling in the California Current with northern areas along the central coast typically experiencing cooler, nutrient-rich water for longer periods of the year (Huyer 1983; Bograd et al. 2009; Bell et al. 2015a). Kelp forests south of Point Conception, in southern California, are subject to lower nutrient conditions, with summer and fall nitrate concentrations falling below  $1 \mu\text{mol L}^{-1}$  (Reed et al. 2011), the concentration below which frond elongation is not sustained (Gerard 1982; Zimmerman and Kremer 1984). We sampled the physiological condition of giant kelp at five kelp forests within this range: Pleasure Point, near Santa Cruz in central California (SC; 36.9564 N, 121.9641 W), Arroyo Quemado (AQ; 34.4677 N, 120.1191 W), Arroyo Burro (AB; 34.4003 N, 119.7446 W), and Mohawk (MO; 34.3941 N, 119.7296 W) in the Santa Barbara Channel, and La Jolla (SD; 32.8532 N, 117.2750 W) near San Diego. The Santa Barbara Channel sites and La Jolla are located within the Southern California Bight. The three sites in the Santa Barbara Channel were sampled monthly by the Santa Barbara Coastal Long Term Ecological Research (SBC LTER) project (August 2012–August 2015), while sites in Santa Cruz and San Diego were sampled quarterly (June 2013–July 2015). On each sample date, 15 mature canopy blades were collected from different individuals. Blades were collected 2 m back from the tip of an actively growing frond to ensure that sampled blades were of a similar age. Blades were placed in a resealable plastic bag and stored in the dark on ice or at 4°C until processed, which occurred within 24 h of collection.

Once at the laboratory, a 5 cm<sup>2</sup> disc was excised from the central portion of each blade, cleaned of epiphytes, and rinsed in a 10% HCl solution to remove any remnants of calcified structures of epiphytes. The 15 discs from each site were combined and weighed to record wet mass, then dried at 60°C for several days, after which, dry mass was recorded.

The combined dried discs were ground to a fine powder using a mortar and pestle and analyzed for carbon content using an elemental analyzer (Carlo-Erba Flash EA 1112 series, Thermo-Finnigan Italia, Milano, Italy). A separate 0.8 cm<sup>2</sup> disc was excised adjacent to the larger disc from each blade for pigment analysis. Each disc selected for pigment analysis was blotted dry and weighed, then placed in 4 mL dimethyl sulfoxide for 45 min at room temperature in the dark. The disc was then removed and rinsed with 1 mL ultrapure water, which was added to the dimethyl sulfoxide extraction, and placed in 5 mL of a mixture of 3 : 1 : 1 acetone, methanol, and ultrapure water for 2 h at 4°C in the dark. Upon removal from the second extract the disc was a pale white color, indicating no remaining pigment (Wheeler 1980). The separate extracts were placed in individual quartz cuvettes and absorbance was measured from 350 nm to 800 nm using a spectrophotometer (Shimadzu UV 2401PC, Tokyo, Japan). Concentrations of Chl and FX were calculated from absorbance at several wavelengths by using empirical equations developed by Seely et al. (1972). Chl:C (mg Chl mg C<sup>-1</sup>) was calculated by dividing the mean mass of Chl by the mean dry mass of carbon, resulting in one Chl:C measurement for each site at each sampling date.

We related changes in giant kelp biomass and production to its physiological condition using data on SFB, frond initiation rate, and NPP collected monthly in permanent plots by the SBC LTER at the three Santa Barbara Channel sites (detailed methods are presented in Rassweiler et al. 2008, 2016). Briefly, each month divers recorded allometric measurements and frond initiation rates of giant kelp plants and the proportion of plants and fronds removed by senescence and disturbance. SFB, defined as the total plant mass excluding the holdfast and reproductive sporophylls, is estimated from empirical allometric relationships between frond number, frond length, and plant wet mass. NPP is calculated as the total amount of biomass produced during the period between each sampling date that explains the observed changes in SFB while accounting for the frond and plant loss rate for that period. This method also incorporates losses due to dissolved and particulate losses from blades by modeling proportional loss rates from canopy and subsurface fronds (Reed et al. 2015; Rassweiler et al. 2016; Rodriguez et al. 2016).

Diver estimates of SFB were not available for Pleasure Point and San Diego. Therefore, we used canopy biomass estimates from the Landsat 7 Enhanced Thematic Mapper Plus and Landsat 8 Operational Land Imager satellites to generate consistent time series of giant kelp canopy dynamics for all five sites (detailed methods in Cavanaugh et al. 2011; Bell et al. 2017). The combination of these two sensors provides an image of the study area every 8 d, with a clear, cloud-free image approximately once a month. Briefly, images were atmospherically corrected and radiometrically standardized using 50 temporally stable pseudo-invariant

targets (85 targets for Landsat 7 images to account for missing data due to the scan line corrector error; Furby and Campbell 2001). Multiple endmember spectral mixing analysis was used to model each 30 × 30 m pixel as a linear combination of two endmembers; one temporally and spatially constant kelp endmember and one of 30 seawater endmembers unique to each image date (Roberts et al. 1998). Multiple seawater endmembers were chosen to account for spatial and temporal differences in water conditions due to sediment plumes, sunglint, and phytoplankton blooms. Kelp canopy biomass was estimated for each pixel using an empirical relationship between diver estimated kelp canopy biomass and modeled fractional kelp cover. A long-term (2002–2015) comparison of Landsat kelp fraction with diver estimated kelp biomass in the Santa Barbara Channel explained 62.4% of canopy biomass dynamics (Cavanaugh et al. 2011; Bell et al. 2017). A monthly time series of kelp canopy biomass was generated for each site over the study period by summing all Landsat pixels within a 100 m radius of each sampling site.

#### Environmental datasets

Spatio-temporal datasets of environmental variables known to be associated with fluctuations in the physiological condition of marine autotrophs were compiled from field measured and remotely sensed sources. In the California Current, as with other coastal upwelling systems, a consistent nonlinear inverse relationship exists between temperature and nutrients, allowing for the estimation of surface nitrate concentration from more spatially and temporally explicit measurements of sea surface temperature (Zimmerman and Kremer 1984; Palacios et al. 2013). We developed a single nonlinear fit between measured surface temperature and nitrate concentrations for the entire study region from coastal oceanographic cruise data collected over 26 yr (< 22 km from the coast; 1990–2015) by California Cooperative Oceanic Fisheries Investigations (CalCOFI; Supporting Information Fig. S1). This temperature/nitrate relationship was validated by estimating nitrate concentration in five SBC LTER kelp forests from *in situ* temperature data compared against nitrate concentrations from water sampled simultaneously ( $r^2 = 0.76$ ;  $p < 0.001$ , Supporting Information Fig. S2). We used this relationship to produce a daily time series of surface nitrate concentrations at each of the five study sites using the nearest 9 km pixel of daily daytime sea surface temperature from the MODIS Aqua satellite sensor from August 2012 to August 2015 (oceandata.sci.gsfc.nasa.gov; see Supporting Information Section S1). Daily mean determinations of photosynthetically active radiation (PAR) at the sea surface at 9 km spatial resolution were obtained from the MODIS Aqua satellite sensor from August 2012 to August 2015 (oceandata.sci.gsfc.nasa.gov).

### Relationship of environment to kelp pigment and physiological condition dynamics

We examined the relationship between known environmental drivers and giant kelp canopy photosynthetic pigment concentrations and Chl:C to assess how changes in available nutrients and light influence the physiological condition of the kelp canopy. We would expect that the effects of variations in ambient nitrate concentration or PAR on the physiological condition of giant kelp will have a temporal lag. We accounted for this by modeling photosynthetic pigments, pigment ratios, carbon content, and Chl:C from all sites as a function of mean nitrate concentration and mean PAR measured for different time periods prior to date that physiological condition variables were measured (1–24 d; Supporting Information Fig. S3). Because there was unequal sampling effort of physiological condition across sites, we randomly resampled the data so that all sites had the same number of pigment, carbon content, and Chl:C measurements (*see* Supporting Information Section S2).

Once the appropriate time lag was found for each predictor variable, we used generalized least squares regressions to model each response variable (Chl, FX, FX:Chl, Chl:C, carbon content) as a function of nitrate and PAR for each region (nlme package; Pinheiro et al. 2016). Generalized least squares regressions were used to account for temporal autocorrelation between the residuals of the model. Beta, or standardized, coefficients were calculated using the `std_beta` function (sjmisc package; Lüdtke 2016). To investigate the nonlinearity of the effects of nitrate concentrations and PAR on the physiological condition of the giant kelp canopy, we used a generalized additive model with a Gaussian error distribution and the identity link function (mgcv package; Wood 2006). This approach models the response variable as the sum of nonlinear functions of several predictor variables. Smoothness parameters were estimated with generalized cross validation. Data were resampled to account for differences in sampling effort across sites and the final model was validated using fivefold cross validation.

### Kelp physiological condition and the dynamics of canopy biomass and NPP

Fluctuations in giant kelp canopy biomass are a function of changing environmental conditions (e.g., seawater nutrient concentrations, surface wave induced disturbance events), intrinsic senescence processes, and the amount of biomass present and available for growth and loss (Reed et al. 2008; Rodriguez et al. 2013; Bell et al. 2015a). To account for the amount of kelp biomass present at the beginning of each season, we assessed changes in canopy biomass through time by examining the residuals of an autoregressive time series model. At each site, we linearly regressed Landsat estimated canopy biomass at time  $t$  by canopy biomass at time  $t - 3$  months. We examined the residuals, which represent the change in kelp biomass over

the season with respect to the starting conditions, and compared these to our time series of site-specific physiological condition using simple linear correlations over time lags of 0–4 months.

Monthly NPP was modeled at the three sites in the Santa Barbara Channel as a function of SFB and/or Chl:C over multiple time lags (0–4 months) using generalized additive models (mgcv package; Wood 2006). The potentially nonlinear relationships between the predictor variables and NPP were examined and model selection was based on the Akaike information criterion. Models were constructed using a Tweedie error structure (power function = 1.1) with a log link and an AR(1) autoregressive model to account for temporal autocorrelation among residuals (mgcv package; Wood 2006). The Tweedie family error structure allows for a variable variance power function to fit the error structure of the data. NPP was predicted from the results of the generalized additive model and compared to the SBC LTER diver-based NPP estimates across sites using a reduced major axis linear regression. Frond initiation rate was also modeled as a function of Chl:C using a reduced major axis linear regression.

## Results

### Spatio-temporal variability in photosynthetic pigments and physiological condition

PAR followed a predictable seasonal cycle at all sites with slight variations among sites due to latitude, clouds, and sampling dates (Fig. 1a). However, the amount of available nitrate in the surface waters varied considerably among the sites throughout the time series. The Santa Cruz site (SC) experienced consistently higher nitrate concentrations in the surface waters throughout the year compared to the southern California sites (Fig. 1b). The Santa Barbara Channel sites (AB, AQ, and MO) experienced periodic increases in nitrate concentrations in the surface waters associated with spring upwelling and low ( $< 1 \mu\text{mol L}^{-1}$ ) concentrations during the summer and fall, while the San Diego site (SD) was characterized by low nitrate concentrations in the surface waters throughout the measurement record. Not surprisingly, fluctuations in Chl and FX pigment concentrations and Chl:C varied by region (Fig. 1c–e). However, carbon content displayed a more erratic pattern through time with little consistent differences by region or season (Fig. 1f). The photosynthetic pigments displayed larger across site variations than carbon content when compared to their means, with a coefficient of variation ( $\sigma/\mu$ ) about twice the magnitude for Chl (0.43) compared to carbon content (0.22).

Photosynthetic pigment dynamics were associated with environmental variables at different magnitudes across the study regions. Concentrations of photosynthetic pigments at the Santa Cruz site were all negatively associated with changes in the amount of PAR and were not significantly related to changes in surface-water nitrate concentrations

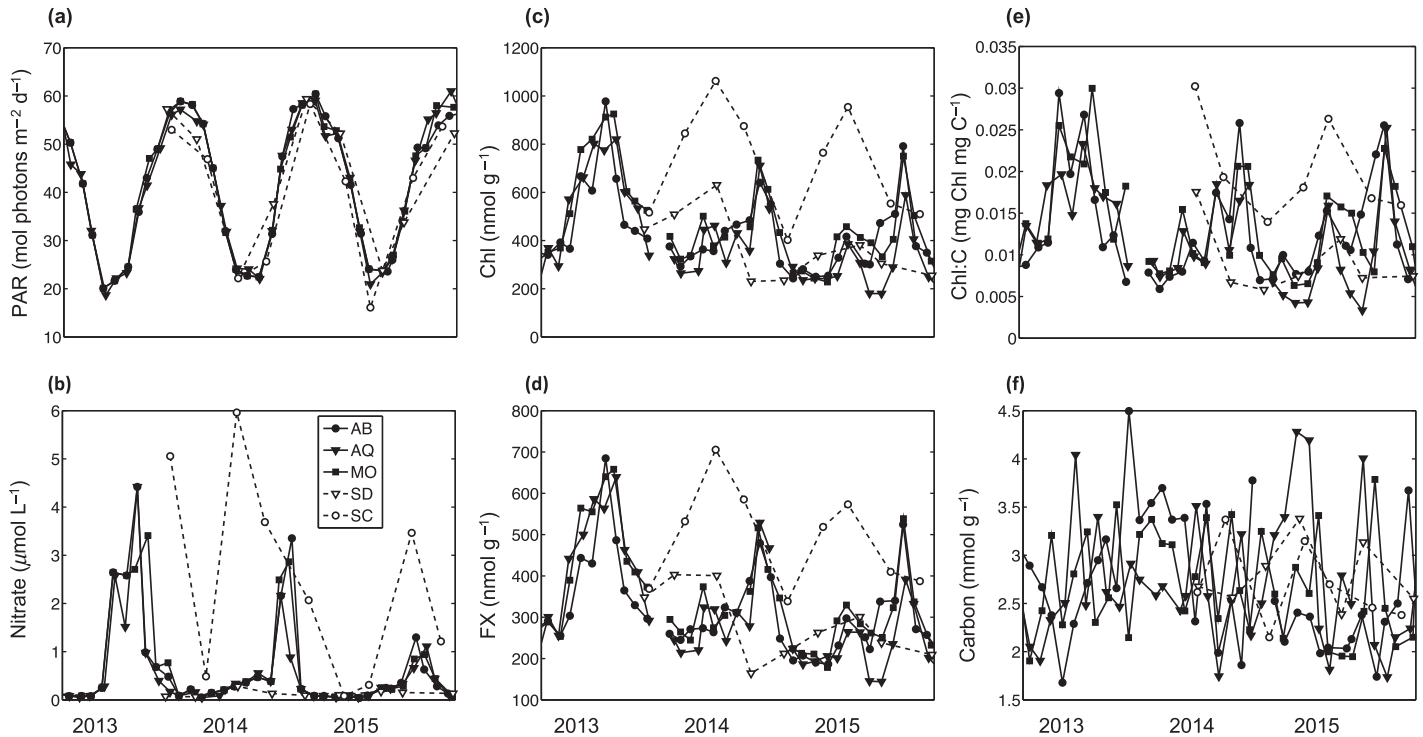


**Fig. 1.** Time series of (a) PAR (18-d mean), and (b) seawater nitrate concentrations (5-d mean) before the sampling date at each site. Time series of (c) Chl, (d) FX, (e) chlorophyll to carbon ratio (Chl:C), and (f) carbon content per gram fresh weight, taken from 15 samples at each of the five study sites: SC, AQ, AB, MO, SD.

(Table 1). This pattern is expected due to high nutrient concentrations at this site. In contrast, pigment concentrations at sites in the Santa Barbara Channel were positively related to changes in nitrate concentration. Chlorophyll *a* and FX concentrations were also negatively related to changes in PAR at the Santa Barbara Channel sites, however, beta coefficient analysis showed that the effect of nitrate concentration was ~3x as great. This pattern is consistent with both nutrient and light availability regulating pigment concentrations at these sites. Changes in pigment concentrations at the San Diego site were not found to be significantly related to either nitrate concentrations or PAR.

The ratio of the two photosynthetic pigments (FX:Chl) was positively related to PAR at the Santa Cruz site, and was positively related to PAR and negatively related to nitrate concentrations at the Santa Barbara Channel sites. Carbon content was not significantly related to changes in nitrate concentrations or PAR at any site. Chlorophyll to carbon ratio was negatively related to PAR at the Santa Cruz site, positively related to nitrate concentrations at the San Diego site, and both negatively related to PAR and positively related to nitrate concentrations at the Santa Barbara Channel sites (Table 1). This antagonistic pattern between nitrate and PAR is expected considering the magnitude and variability of surface nitrate concentrations at the three sites.

**Table 1.** Beta (standardized) coefficients of the photosynthetic pigments chlorophyll *a* (Chl) and FX, pigment ratio (FX:Chl), carbon content, and chlorophyll to carbon ratio (Chl:C) in relation to changes in nitrate concentration (NO<sub>3</sub>) and PAR at each site. Bold values are significant at  $\alpha = 0.05$ .

Site		Chl	FX	FX:Chl	Carbon	Chl:C
Santa Cruz <i>n</i> = 9	NO <sub>3</sub>	-0.06	0.03	-0.49	-0.21	0.18
	PAR	<b>-0.89</b>	<b>-0.86</b>	<b>0.64</b>	0.45	<b>-0.82</b>
SBC <i>n</i> = 111	NO <sub>3</sub>	<b>0.69</b>	<b>0.71</b>	<b>-0.25</b>	-0.02	<b>0.50</b>
	PAR	<b>-0.24</b>	<b>-0.21</b>	<b>0.29</b>	0.04	<b>-0.28</b>
San Diego <i>n</i> = 9	NO <sub>3</sub>	0.39	0.24	-0.39	-0.99	<b>1.00</b>
	PAR	-0.03	0.02	0.35	-0.67	0.06

Values of Chl:C of the surface canopy, combined from across all five sites, were modeled as nonlinear functions of both surface-water nitrate concentration and PAR and were significantly related to both variables ( $R^2 = 0.70$ ;  $p < 0.001$ ;  $n = 120$ ). Concentrations of nitrate below 0.5 μmol L<sup>-1</sup> are difficult to estimate from high seawater temperature due to the variability in the nitrogen depletion temperature. Nevertheless, Chl:C was negatively related to nitrate at low concentrations (0–0.5 μmol L<sup>-1</sup>), but showed an increasingly positive relationship up to ~ 1.5 μmol L<sup>-1</sup> (Fig. 2a). There was a stable positive relationship between nitrate concentration and

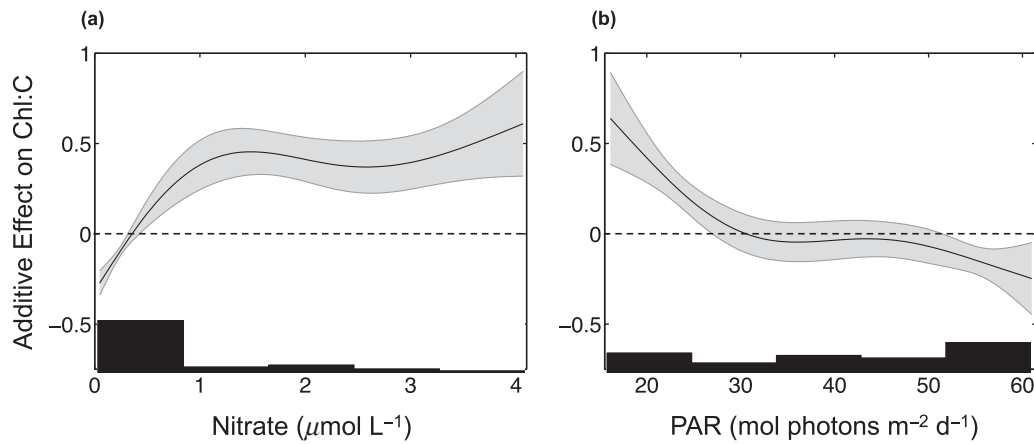


**Fig. 2.** Nonlinear additive effect curves of (a) seawater nitrate concentration and (b) PAR on the chlorophyll to carbon ratio (Chl:C) of giant kelp canopy blades across all sites. The solid line is the mean effect of the predictor and the shaded regions represent the standard error. The frequency of each predictor variable through space and time is shown as the black histogram at the bottom of each plot. The dashed line represents zero effect above which the predictor will have a positive effect on Chl:C and below which the predictor will have a negative effect.

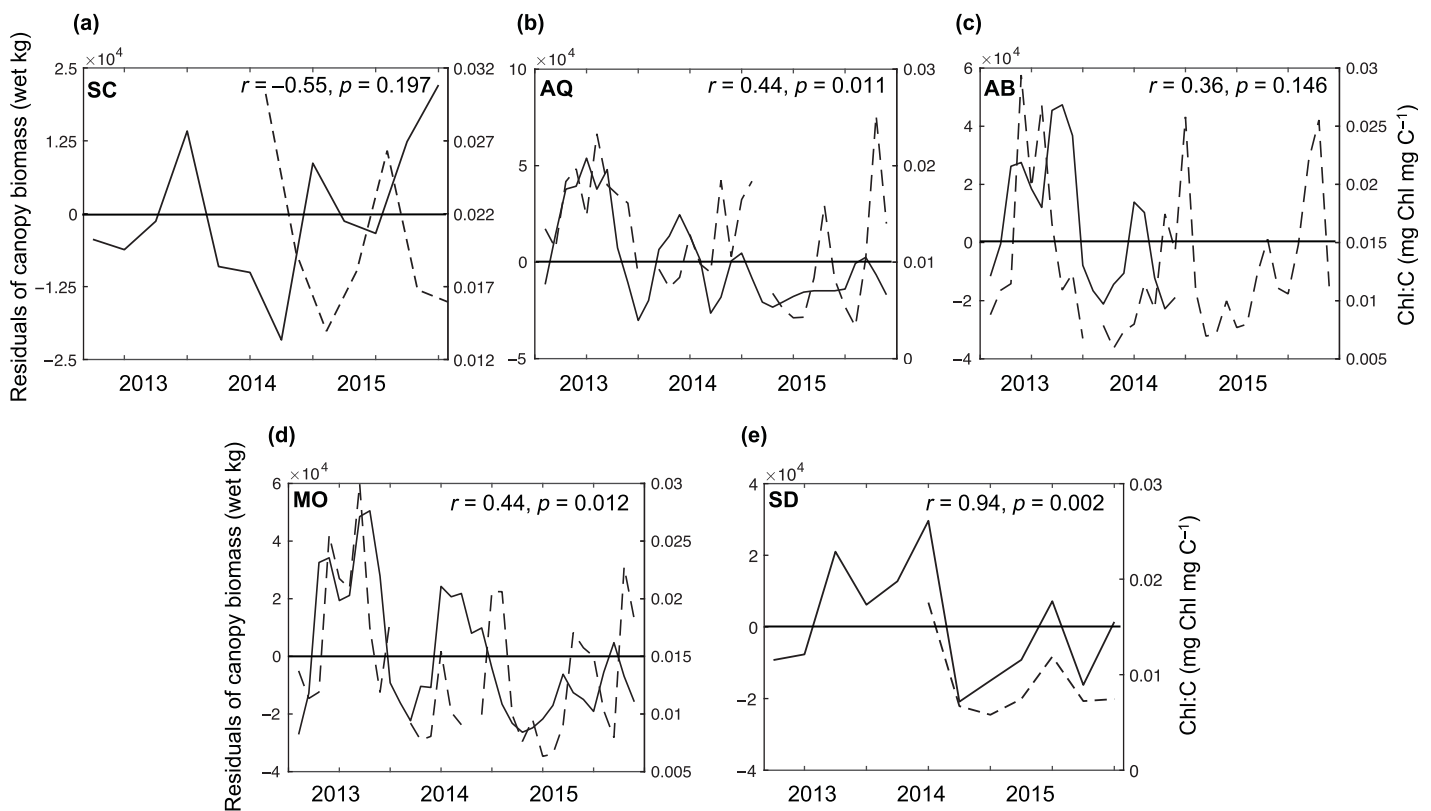


**Fig. 3.** Residual canopy biomass after removing 3-month autocorrelation of all Landsat pixels ( $30 \times 30$  m) within 100 m to the study site (solid line) and chlorophyll to carbon ratio (Chl:C; dashed line) for the five study sites: (a) SC, (b) AQ, (c) AB, (d) MO, (e) SD. Pearson correlation coefficients ( $r$ ) and calculated probabilities ( $p$ ) reported for linear correlation between residuals and 3-month lagged Chl:C for each site through time.

Chl:C from  $1.5 \mu\text{mol L}^{-1}$  to  $4 \mu\text{mol L}^{-1}$ . PAR showed a strong negative correlation with Chl:C at  $15 \text{ mol photons m}^{-2} \text{ d}^{-1}$  to  $\sim 30 \text{ mol photons m}^{-2} \text{ d}^{-1}$  and a weaker negative correlation as values increased beyond  $\sim 50 \text{ mol photons m}^{-2} \text{ d}^{-1}$  (Fig. 2b).

### Relationship between canopy biomass dynamics and physiological condition

To determine changes in giant kelp canopy, we used Landsat imagery to generate a canopy biomass time series for each site. The degree of temporal autocorrelation of

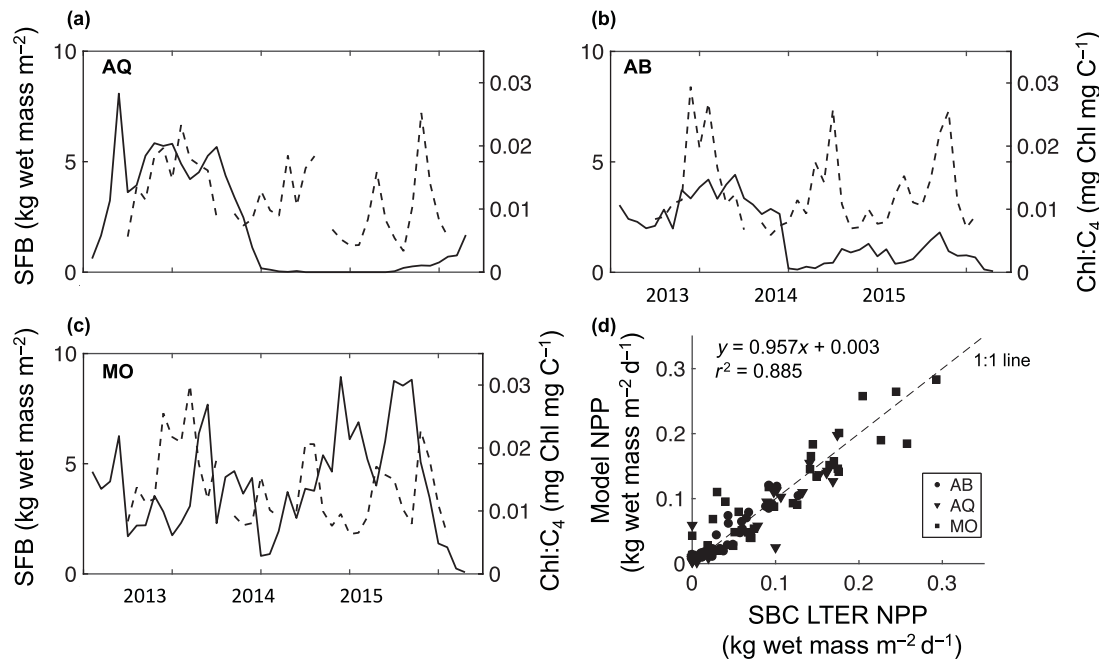


**Fig. 4.** SFB (solid line) and 4-month lagged chlorophyll to carbon ratio (Chl:C<sub>4</sub>; dashed line) time series for each site in the Santa Barbara Channel, (a) AQ, (b) AB, and (c) MO, (d) NPP estimated from SBC LTER project diver data at multiple time points and modeled NPP from diver estimated SFB and Chl:C<sub>4</sub>. The statistics represent the coefficient of determination ( $r^2$ ) and reduced major axis linear regression equation between SBC LTER estimated NPP and the NPP model discussed in this paper which incorporates SFB and temporally lagged Chl:C.

canopy biomass showed differences between the central and southern California sites. Canopy biomass three months prior to a given time point explained about one fourth of the variation in canopy biomass at the three Santa Barbara Channel sites, AQ ( $r^2 = 0.20$ ;  $p < 0.01$ ;  $n = 34$ ), AB ( $r^2 = 0.27$ ;  $p < 0.01$ ;  $n = 19$ ), MO ( $r^2 = 0.23$ ;  $p < 0.01$ ;  $n = 34$ ), and the San Diego site ( $r^2 = 0.25$ ;  $p = 0.10$ ;  $n = 9$ ), while explaining little variation at the Santa Cruz site ( $r^2 = 0.05$ ;  $p = 0.48$ ;  $n = 9$ ).

The canopy biomass residuals of these temporal autocorrelation functions tended to be negative in the winter and positive in the summer at the Santa Cruz site (Fig. 3a), while sites in southern California displayed much interannual variability in biomass change (Fig. 3b–e). Residuals were not significantly related to Chl:C at the Santa Cruz site, however, Chl:C was significantly and positively related to residuals at two of the Santa Barbara Channel sites, and the San Diego site with a temporal lag time of three months. Residuals from the AB site were not available after April 2014 as canopy biomass was too low to be quantified by the Landsat sensor resulting in only 19 months of canopy biomass residuals vs. 34 months at the other Santa Barbara Channel sites.

#### Relationship between NPP and physiological condition

At the three Santa Barbara Channel sites, values of Chl:C were positively and significantly related to the initiation rate of giant kelp fronds recorded by SBC LTER divers ( $r^2 = 0.14$ ;  $p < 0.001$ ;  $n = 97$ ; Supporting Information Fig. S4), confirming that canopy Chl:C was a useful proxy for kelp physiological condition. Time series of SFB and temporally lagged (4-

months) Chl:C<sub>4</sub> were used to model NPP and assess nonlinear relationships at the three sites in the Santa Barbara Channel (Fig. 4a–c). Predictions of NPP based solely on SFB and 4-month temporally lagged Chl:C closely matched those of the SBC LTER estimates of NPP ( $y = 0.957x + 0.003$ ;  $r^2 = 0.885$ ;  $p < 0.0001$ ; root mean square error (RMSE) = 0.023;  $n = 106$ ; Fig. 4d).

The relationship between SFB and field estimated NPP was asymptotic and increased linearly as SFB increased from 0 kg wet mass m<sup>-2</sup> to 3 kg wet mass m<sup>-2</sup> ( $p < 0.0001$ ; Fig. 5a; Supporting Information Table S1). The relationship was initially negative at low biomass and became positive at 2 kg wet mass m<sup>-2</sup>, and reached an asymptote from 3 kg wet mass m<sup>-2</sup> to 9 kg wet mass m<sup>-2</sup>. Temporally lagged (4-months) chlorophyll to carbon ratio (Chl:C<sub>4</sub>) was significantly related to NPP ( $p = 0.0014$ ; Supporting Information Table S1). There was a negative additive effect on NPP when the Chl:C<sub>4</sub> was below 0.007 mg Chl mg C<sup>-1</sup> (Fig. 5b). Using Chl:C<sub>4</sub> and SFB as predictors of NPP improved the model fit, and increased model parsimony by reducing the Akaike information criterion from  $-282.22$  to  $-296.99$ , vs. using SFB as the sole predictor variable.

#### Discussion

##### Environmental variation as drivers of photosynthetic pigment state and physiological condition

Understanding the effect of physiological condition on the dynamics of giant kelp is challenging as the variability

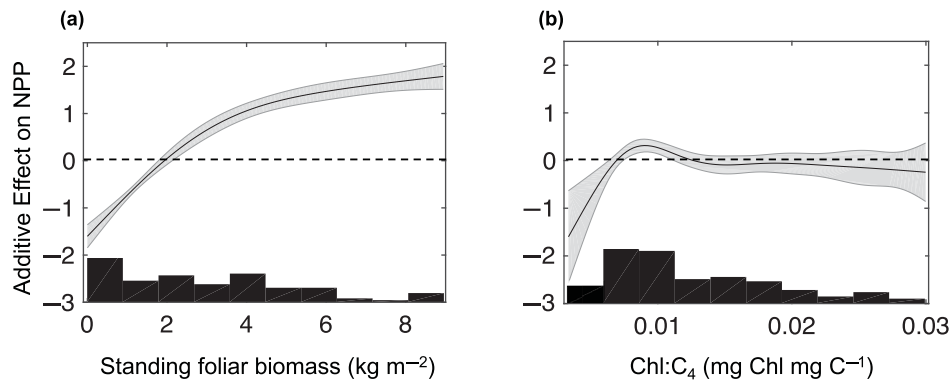


**Fig. 5.** Additive effect curves of **(a)** SFB and **(b)** 4-month lagged chlorophyll to carbon ratio (Chl:C<sub>4</sub>) on the NPP of giant kelp across the three sites in the Santa Barbara Channel. The solid line is the mean effect of the predictor and the shaded regions represent the standard error. The frequency of each predictor variable through space and time is shown as the black histogram at the bottom of each plot. The dashed line represents zero effect above which the predictor will have a positive effect on NPP and below which the predictor will have a negative effect.

of this foundational species is controlled by a combination of top-down, bottom-up, and disturbance forces (Reed et al. 2011; Bell et al. 2015a; Schiel and Foster 2015). One way to begin to tease apart these environmental effects on physiological condition is to examine changes in photosynthetic pigments and other physiological proxies over gradients of environmental conditions. Giant kelp in the NE Pacific spans a broad range of light and nutrient environments, from the large seasonal light fluctuations of SE Alaska to the warm, relatively nutrient-poor waters of southern California and Baja California (Graham et al. 2007). We should expect this species to adjust its photosynthetic pigment concentrations according to its local environmental conditions.

During nutrient-replete conditions, many marine autotrophs increase their photosynthetic pigment concentrations under low light conditions and decrease pigment concentrations during periods of high light (e.g., Wiginton and McMillan 1979). It is not surprising then that fluctuations in photosynthetic pigments at Santa Cruz were strongly and negatively associated with changes in PAR rather than nutrients, which occur at relatively high concentrations throughout most of the year (Table 1). Kelp canopy pigments in the Santa Barbara Channel showed a different pattern than the northern Santa Cruz site, as relatively high pigment levels were sometimes observed during periods of high light availability. Pigment concentrations more closely mirrored seasonal and interannual variation in nitrate concentrations in the more oligotrophic waters of the Santa Barbara Channel. However, pigment concentrations alone were not significantly related to either nitrate concentrations or PAR at the San Diego site.

The ratio of the accessory photosynthetic pigment FX to Chl may highlight an additional photoprotective function, as it was positively associated with PAR. While other accessory pigments have shown a negative relationship to light levels, FX:Chl is an exception to this rule in other brown macroalgae and diatoms (Brown and Richardson 1968). Carotenoid

pigments like FX are light-harvesting pigments, however, they can also exert a protective effect against photooxidation of cell material in high light environments, so this positive association with PAR may be a response to the increased light levels in the canopy (Clayton 1980; Di Valentin et al. 2012).

Patterns of Chl:C were associated with nutrient and light dynamics at different magnitudes across the study regions. Seawater nitrate concentration had an increasingly positive relationship with the physiological condition of kelp along a north to south gradient as nutrient limitation became more prevalent (Table 1). While the photosynthetic pigments from the San Diego site did not show a significant relationship to PAR or nitrate concentrations, there was a significant and positive relationship between nitrate concentration and Chl:C despite the small sample size. These differences in the magnitude of the relationships of nitrate concentration and PAR to the Chl:C of the kelp canopy are likely the result of nonlinear effects (Fig. 2a). The sharp increase in Chl:C at nitrate concentrations between  $0 \mu\text{mol L}^{-1}$  and  $1.5 \mu\text{mol L}^{-1}$  is consistent with previous studies that have shown the growth rate of juvenile kelp plants and the elongation rate of mature fronds increased rapidly over this range (Gerard 1982; Zimmerman and Kremer 1984, 1986; Kocczak et al. 1991; Brzezinski et al. 2013). The small effect size of PAR for all but the lowest observed PAR values suggests that light limitation only influences the Chl:C of the giant kelp canopy in California during the winter months, however, this effect may be more prevalent at higher latitudes (Fig. 2b). The negative effect of PAR on Chl:C was evidenced by lower Chl:C values during the summer at all sites, and may reflect the canopy's need for less photosynthetic pigment to maintain growth at higher light levels.

### The role of physiological condition in giant kelp dynamics

Giant kelp canopy biomass tends to be autocorrelated at a seasonal scale due to temporally lagged intrinsic processes such as age-dependent mortality of fronds that limits their

lifespans to  $\sim 100$  d (Rodriguez et al. 2013; Bell et al. 2015a). Temporal autocorrelation explained a greater proportion of kelp canopy biomass in southern California compared to central California as the more exposed central California coastline experiences pronounced winter wave disturbance leading to abrupt changes in canopy biomass (Reed et al. 2011; Bell et al. 2015a,b). Deviations from the previous biomass state are indicative of processes affecting the growth, loss, or demography of giant kelp plants and fronds. These changes in canopy biomass were not positively related to Chl:C at Santa Cruz as high pigment levels in winter coincided with low canopy biomass (Fig. 3a).

The positive relationship between changes in canopy biomass and Chl:C that we observed in southern California (two of three Santa Barbara Channel sites and the SD site) indicates that the physiological state of the canopy is associated with giant kelp biomass dynamics in these periodically nutrient limited systems (Fig. 3b–e). Changes in canopy biomass result from autocorrelated demographic processes as well as fluctuating environmental conditions that influence its physiological state. For instance, high rates of frond elongation resulting from an increase in externally supplied nutrients can lead to a rapid accumulation of canopy biomass as fronds grow and reach the surface or add to their surface length (Zimmerman and Kremer 1986). The biomass of canopy fronds, however, is also controlled by progressive senescence that occurs independently of ambient nutrient conditions (Rodriguez et al. 2013). As a result, fluctuations in canopy biomass may appear independent of concurrent fluctuations in environmental conditions that affect its physiological state, even in the absence of disturbances that physically remove fronds.

The SBC LTER time series of giant kelp NPP relies on *in situ* measurements of changes in SFB from one period to the next, while simultaneously constraining processes that account for biomass losses due to plant and frond mortality, blade senescence, and exudation (Fig. 4a–c; Rassweiler et al. 2008, 2016; Reed et al. 2015). Simplifying the estimation of NPP to a function of the SFB state and lagged Chl:C, removes the need to quantify these loss terms and compared well with this more comprehensive method (Fig. 4d). Modeling NPP as a function of biomass and physiological condition opens the possibility of NPP estimates over large spatial scales with available and/or future remotely sensed products (discussed below).

Modeling giant kelp NPP from SFB and temporally lagged Chl:C required knowledge of each variable's relationship to NPP. We found a positive and asymptotic relationship between SFB and NPP (Fig. 5a). One possible explanation for the asymptotic nature of this relationship is a reduction in photosynthesis due to density dependent shelf shading as the size and biomass of the forest increases. This is consistent with the negative relationship between specific growth rate and SFB that was observed at the Santa Barbara Channel

sites by Reed et al. (2008). Additional support for this hypothesis comes from Stewart et al. (2009) who found that canopy fronds growing at the offshore edge of the Mohawk kelp forest in the Santa Barbara Channel displayed a higher elongation rate than interior canopy fronds. Since giant kelp grows on limited areas of rocky reef, biomass may be added without any increase in edge area as the reef nears carrying capacity.

The relationship of Chl:C to NPP may be both a function of the production of growing fronds as well as frond initiation. Frond initiation rate was related to Chl:C, with low or zero initiation only occurring at canopy Chl:C values less than  $0.011 \text{ mg Chl mg C}^{-1}$  (Supporting Information Fig. S4). Fox (2016) found that a reduction in canopy biomass decreases frond initiation through a decline of photosynthate transport to the deeper areas near the holdfast where frond initiation occurs. If growing canopy fronds are in a poor physiological state due to nutrient limitation, then photosynthesis is reduced and frond initiation declines. A lack of frond initiation will be most consequential to NPP in the forthcoming months when a greater proportion of fronds are senescing, displaying decreased tissue integrity and photosynthetic capacity (Rodriguez et al. 2016; Stephens and Hepburn 2016). Low Chl:C in growing fronds may signal a forest that will be primarily composed of senescing fronds in 4-months' time. A forest composed of senescing fronds may present a high standing biomass, but have little photosynthetic capacity to generate commensurate levels of NPP. Therefore, the age-structure of fronds in the kelp canopy may be critically important to overall production. While this study focused on the Chl:C of growing fronds, future studies may wish to characterize the physiological condition of all canopy fronds to gain a better understanding of the links between kelp photosynthetic state and frond dynamics through time.

#### Estimation of NPP from remotely sensed observations

Recent advances in the remote estimation of giant kelp biomass have revealed how biomass dynamics are associated with changes in environmental conditions (Cavanaugh et al. 2011; Bell et al. 2015a). Currently, Landsat multispectral imagery is used to estimate canopy biomass of giant kelp forests in the NE Pacific (Cavanaugh et al. 2011; Bell et al. 2017), while canopy Chl:C can be assessed from high spectral resolution ( $\sim 10$  nm; hyperspectral) visible imagery (Bell et al. 2015b). Combining these estimates of canopy biomass along with spatially explicit canopy Chl:C could potentially lead to regional time series of giant kelp NPP. The inclusion of physiological condition in this estimation is important, as hyperspectral imagery has shown up to a twofold difference in Chl:C across a single kelp forest when moving from the inshore to offshore edge (Bell et al. 2015b). While global hyperspectral imagery is currently unavailable, the planned Hyperspectral Infrared Imager mission would provide repeat

hyperspectral imagery on the appropriate spatial scales for estimating both giant kelp canopy biomass and physiological condition simultaneously, thereby making NPP estimates of giant kelp available on a global scale (Bell et al. 2015b; Hochberg et al. 2015; Lee et al. 2015).

We have shown that the physiological condition of giant kelp canopy blades is a predictable function of sea surface nitrate concentrations and PAR, with both variables estimated from satellite imagery. The use of subregional (~ 4 – 9 km resolution) satellite remote sensing estimates of PAR and nitrate concentration at the sea surface could be used to estimate canopy Chl:C. These estimates of Chl:C could be combined with Landsat estimates of kelp canopy biomass to generate time series of NPP for the entire range of giant kelp in California and Baja California, Mexico, using relationships validated with NPP estimates from the SBC. Such regional estimates of giant kelp NPP would be useful for informing many active areas of research including food web dynamics, carbon export, demographic connectivity, and the impacts of climate change (Dugan et al. 2003; Byrnes et al. 2011; Morton et al. 2016; Castorani et al. 2017).

Changes in photosynthetic pigment concentrations and the physiological condition of giant kelp canopy are associated with fluctuations in environmental conditions; however, the strength of these associations varies regionally. Many of these processes linking physiological condition to biomass accumulation, and thus NPP, are integrated over varied timescales, and translate to measurable changes over the course of several months. By leveraging the present state of kelp forest biomass, along with knowledge of the physiological state of the canopy, it may be possible to generate spatially expansive time series of NPP for this important foundation species.

## References

- Behrenfeld, M. J., E. Boss, D. A. Siegel, and D. M. Shea. 2005. Carbon-based ocean productivity and phytoplankton physiology from space. *Global Biogeochem. Cycles* **19**: 1–14. doi:10.1029/2004GB002299
- Bell, T. W., K. C. Cavanaugh, D. C. Reed, and D. A. Siegel. 2015a. Geographical variability in the controls of giant kelp biomass dynamics. *J. Biogeogr.* **42**: 2010–2021. doi:10.1111/jbi.12550
- Bell, T. W., K. C. Cavanaugh, and D. A. Siegel. 2015b. Remote monitoring of giant kelp biomass and physiological condition: An evaluation of the potential for the Hyperspectral Infrared Imager (HyspIRI) mission. *Remote Sens. Environ.* **167**: 218–228. doi:10.1016/j.rse.2015.05.003
- Bell, T. W., K. C. Cavanaugh, and D. A. Siegel. 2017. SBC LTER: Time series of quarterly NetCDF files of kelp biomass in the canopy from Landsat 5, 7 and 8, 1984 – 2016 (ongoing). Santa Barbara Coastal LTER.
- Bograd, S. J., I. Schroeder, N. Sarkar, X. Qiu, W. J. Sydeman, and F. B. Schwing. 2009. Phenology of coastal upwelling in the California Current. *Geophys. Res. Lett.* **36**: 1602. doi:10.1029/2008GL035933
- Brown, T. E., and F. L. Richardson. 1968. The effect of growth environment on the physiology of algae: Light intensity. *J. Phycol.* **4**: 38–54. doi:10.1111/j.1529-8817.1968.tb04675.x
- Brzezinski, M., D. Reed, S. Harrer, A. Rassweiler, J. M. Melack, B. M. Goodridge, and J. E. Dugan. 2013. Multiple sources and forms of nitrogen sustain year-round kelp growth on the inner continental shelf of the Santa Barbara Channel. *Oceanography* **26**: 114–123. doi:10.5670/oceanog.2013.53
- Byrnes, J., D. Reed, B. Cardinale, K. Cavanaugh, S. Holbrook, and R. Schmitt. 2011. Climate driven increases in storm frequency simplify kelp forest food webs. *Glob. Chang. Biol.* **17**: 2513–2524. doi:10.1111/j.1365-2486.2011.02409.x
- Castorani, M. C., D. C. Reed, P. T. Raimondi, F. Alberto, T. W. Bell, K. C. Cavanaugh, D. A. Siegel, and R. Simons. 2017. Fluctuations in population fecundity drive variation in demographic connectivity and metapopulation dynamics. *Proc. Royal Soc. B* **284**: 20162086. doi:10.1098/rspb.2016.2086
- Cavanaugh, K. C., D. A. Siegel, D. C. Reed, and P. E. Dennison. 2011. Environmental controls of giant-kelp biomass in the Santa Barbara Channel, California. *Mar. Ecol. Prog. Ser.* **429**: 1–17. doi:10.3354/meps09141
- Clayton, R. K. 1980. *Photosynthesis: Physical mechanisms and chemical patterns*. Cambridge Univ. Press.
- Colombo-Pallotta, M. F., E. García-Mendoza, and L. B. Ladah. 2006. Photosynthetic performance, light absorption, and pigment composition of *Macrocystis pyrifera* (Laminariales, Phaeophyceae) blades from different depths. *J. Phycol.* **42**: 1225–1234. doi:10.1111/j.1529-8817.2006.00287.x
- Dayton, P. K., M. J. Tegner, P. E. Parnell, and P. B. Edwards. 1992. Temporal and spatial patterns of disturbance and recovery in a kelp forest community. *Ecol. Monogr.* **62**: 421–445. doi:10.2307/2937118
- Di Valentin, M., C. Büchel, G. M. Giacometti, and D. Carbonera. 2012. Chlorophyll triplet quenching by fucoxanthin in the fucoxanthin-chlorophyll protein from the diatom *Cyclotella meneghiniana*. *Biochem. Biophys. Res. Commun.* **427**: 637–41. doi:10.1016/j.bbrc.2012.09.113
- Dugan, J. E., D. M. Hubbard, M. D. McCrary, and M. O. Pierson. 2003. The response of macrofauna communities and shorebirds to macrophyte wrack subsidies on exposed sandy beaches of southern California. *Estuar. Coast. Shelf Sci.* **58**: 25–40. doi:10.1016/S0272-7714(03)00045-3
- Fox, M. 2016. Biomass loss reduces growth and resource translocation in giant kelp *Macrocystis pyrifera*. *Mar. Ecol. Prog. Ser.* **562**: 65–77. doi:10.3354/meps11949
- Furby, S. L., and N. A. Campbell. 2001. Calibrating images from different dates to “like-value” digital counts. *Remote Sens. Environ.* **77**: 186–196. doi:10.1016/S0034-4257(01)00205-X

- Geider, R. J. 1987. Light and temperature dependence of the carbon to chlorophyll *a* ratio in microalgae and cyanobacteria: Implications for physiology and growth of phytoplankton. *New Phytol.* **106**: 1–34. doi:10.1111/j.1469-8137.1987.tb04788.x
- Gerard, V. A. 1982. Growth and utilization of internal nitrogen reserves by the giant kelp *Macrocystis pyrifera* in a low-nitrogen environment. *Mar. Biol.* **66**: 27–35. doi:10.1007/BF00397251
- Graham, M. H., J. A. Vásquez, and Buschmann, A. H. 2007. Global ecology of the giant kelp *Macrocystis*: From ecotypes to ecosystems, p. 39–88. *In* Oceanography and marine biology: An annual review, v. 45. CRC Press.
- Hochberg, E. J., D. A. Roberts, P. E. Dennison, and G. C. Hulley. 2015. Remote sensing of environment special issue on the Hyperspectral Infrared Imager (HyspIRI): Emerging science in terrestrial and aquatic ecology, radiation balance and hazards. *Remote Sens. Environ.* **167**: 1–5. doi:10.1016/j.rse.2015.06.011
- Huyer, A. 1983. Coastal upwelling in the California current system. *Prog. Oceanogr.* **12**: 259–284. doi:10.1016/0079-6611(83)90010-1
- Kirk, J. T. O. 1994. Light and photosynthesis in aquatic ecosystems. Cambridge Univ. Press.
- Kopczak, C. D. 1994. Variability of nitrate uptake capacity in *Macrocystis pyrifera* (Laminariales, Phaeophyta) with nitrate and light availability. *J. Phycol.* **30**: 573–580. doi:10.1111/j.0022-3646.1994.00573.x
- Kopczak, C. D., R. C. Zimmerman, and J. N. Kremer. 1991. Variation in nitrogen physiology and growth among geographically isolated populations of the giant kelp, *Macrocystis pyrifera* (Phaeophyta). *J. Phycol.* **27**: 149–158. doi:10.1111/j.0022-3646.1991.00149.x
- Laws, E., and T. Bannister. 1980. Nutrient and light-limited growth of *Thalassiosira fluviatilis* in continuous culture, with implications for phytoplankton growth in the ocean. *Limnol. Oceanogr.* **25**: 457–473. doi:10.4319/lo.1980.25.3.0457
- Lee, C. M., M. L. Cable, S. J. Hook, R. O. Green, S. L. Ustin, D. J. Mandl, and E. M. Middleton. 2015. An introduction to the NASA Hyperspectral InfraRed Imager (HyspIRI) mission and preparatory activities. *Remote Sens. Environ.* **167**: 6–19. doi:10.1016/j.rse.2015.06.012
- Leet, W. S., C. M. Dewees, R. Klingbeil, and E. J. Johnson. 2001. California's living marine resources: A status report, p. 593. State of CA Resources Agency and Fish and Game.
- Lüdecke, D. 2016. sjmisc: Miscellaneous data management tools. R package version 1.7.
- Morton, D. N., T. W. Bell, and T. W. Anderson. 2016. Spatial synchrony of amphipods in giant kelp forests. *Mar. Biol.* **163**: 32. doi:10.1007/s00227-015-2807-5
- Palacios, D. M., E. L. Hazen, I. D. Schroeder, and S. J. Bograd. 2013. Modeling the temperature-nitrate relationship in the coastal upwelling domain of the California Current. *J. Geophys. Res. Oceans* **118**: 3223–3239. doi:10.1002/jgrc.20216
- Pinheiro, J., D. Bates, S. DebRoy, D. Sarkar, and R Core Team. 2016. nlme: Linear and nonlinear mixed effects models. R package version 3.1–127.
- Rassweiler, A., K. K. Arkema, and D. C. Reed. 2008. Net primary production, growth, and standing crop of *Macrocystis pyrifera* in Southern California. *Ecology* **89**: 2068. doi:10.1890/07-1109.1
- Rassweiler, A., K. Arkema, D. C. Reed, R. C. Zimmerman, and M. A. Brzezinski. 2016. SBC LTER: Reef: Net primary production, growth and standing crop of *Macrocystis pyrifera* in Southern California. Santa Barbara Coastal LTER.
- Reed, D. C., B. P. Kinlan, P. T. Raimondi, L. Washburn, B. Gaylord, and P. T. Drake. 2006. A metapopulation perspective on patch dynamics and connectivity of giant kelp, p. 352–386. *In* J. P. Kritzer and P. F. Sale [eds.], Marine metapopulations. Academic Press.
- Reed, D. C., A. Rassweiler, and K. K. Arkema. 2008. Biomass rather than growth rate determines variation in net primary production by giant kelp. *Ecology* **89**: 2493–2505. doi:10.1890/07-1106.1
- Reed, D. C., A. Rassweiler, M. H. Carr, K. C. Cavanaugh, D. P. Malone, and D. A. Siegel. 2011. Wave disturbance overwhelms top-down and bottom-up control of primary production in California kelp forests. *Ecology* **92**: 2108–2116. doi:10.1890/11-0377.1
- Reed, D. C., C. A. Carlson, E. R. Halewood, J. C. Nelson, S. L. Harrer, A. Rassweiler, and R. J. Miller. 2015. Patterns and controls of reef-scale production of dissolved organic carbon by giant kelp *Macrocystis pyrifera*. *Limnol. Oceanogr.* **60**: 1996–2008. doi:10.1002/lno.10154
- Roberts, D. A., M. Gardner, R. Church, S. Ustin, G. Scheer, and R. O. Green. 1998. Mapping chaparral in the Santa Monica Mountains using multiple endmember spectral mixture models – II. Environmental influences on regional abundance. *Remote Sens. Environ.* **65**: 267–279. doi:10.1016/S0034-4257(98)00037-6
- Rodriguez, G. E., A. Rassweiler, D. C. Reed, and S. J. Holbrook. 2013. The importance of progressive senescence in the biomass dynamics of giant kelp (*Macrocystis pyrifera*). *Ecology* **94**: 1848–1858. doi:10.1890/12-1340.1
- Rodriguez, G. E., D. C. Reed, and S. J. Holbrook. 2016. Blade life span, structural investment, and nutrient allocation in giant kelp. *Oecologia* **182**: 397–404. doi:10.1007/s00442-016-3674-6
- Sakshaug, E., K. Andresen, and D. Kiefer. 1989. A steady state description of growth and light absorption in the marine planktonic diatom *Skeletonema costatum*. *Limnol. Oceanogr.* **34**: 198–205. doi:10.4319/lo.1989.34.1.0198
- Schiel, D. R., and M. S. Foster. 2015. The biology and ecology of giant kelp forests. Univ. of California Press.
- Seely, G., M. Duncan, and W. Vidaver. 1972. Preparative and analytical extraction of pigments from brown algae with

- dimethyl sulfoxide. *Mar. Biol.* **12**: 184–188. doi:[10.1007/BF00350754](https://doi.org/10.1007/BF00350754)
- Shivji, M. S. 1984. Physiological responses of juvenile *Macrocystis pyrifera* sporophytes (Phaeophyta) to environmental factors: Light, nitrogen and the interaction of light and nitrogen, p. 51. M.A. thesis in biology. Univ. of California.
- Shivji, M. S. 1985. Interactive effects of light and nitrogen on growth and chemical composition of juvenile *Macrocystis pyrifera* (L.) C. Ag. (Phaeophyta) sporophytes. *J. Exp. Mar. Biol. Ecol.* **89**: 81–96. doi:[10.1016/0022-0981\(85\)90083-8](https://doi.org/10.1016/0022-0981(85)90083-8)
- Stephens, T. A., and C. D. Hepburn. 2016. A kelp with integrity: *Macrocystis pyrifera* prioritises tissue maintenance in response to nitrogen fertilisation. *Oecologia* **181**: 1–14. doi:[10.1007/s00442-016-3641-2](https://doi.org/10.1007/s00442-016-3641-2)
- Stewart, H., J. Fram, and D. Reed. 2009. Differences in growth, morphology and tissue carbon and nitrogen of *Macrocystis pyrifera* within and at the outer edge of a giant kelp forest in California, USA. *Mar. Ecol. Prog. Ser.* **375**: 101–112. doi:[10.3354/meps07752](https://doi.org/10.3354/meps07752)
- Wheeler, W. N. 1980. Pigment content and photosynthetic rate of the fronds of *Macrocystis pyrifera*. *Marine Biology* **56**: 97–102.
- Wiginton, J. R., and C. McMillan. 1979. Chlorophyll composition under controlled light conditions as related to the distribution of seagrasses in Texas and the U.S. Virgin Islands. *Aquat. Bot.* **6**: 171–184. doi:[10.1016/0304-3770\(79\)90060-3](https://doi.org/10.1016/0304-3770(79)90060-3)
- Wood, S. N. 2006. Generalized additive models: An introduction with R. Chapman and Hall/CRC.
- Zimmerman, R. C., and J. N. Kremer. 1984. Episodic nutrient supply to a kelp forest ecosystem in Southern California. *J. Mar. Res.* **42**: 591–604. doi:[10.1357/002224084788506031](https://doi.org/10.1357/002224084788506031)
- Zimmerman, R. C., and J. N. Kremer. 1986. *In situ* growth and chemical composition of the giant kelp, *Macrocystis pyrifera*: Response to temporal changes in ambient nutrient availability. *Mar. Ecol. Prog. Ser.* **27**: 277–285. doi:[10.3354/meps027277](https://doi.org/10.3354/meps027277)

### Acknowledgments

We would like to acknowledge the support of the US National Science Foundation which provided funding for the Santa Barbara Coastal LTER (OCE 0620276 and 1232779). We would also like to thank NASA for its support of TWB through the Earth and Space Science Fellowship program and through NASA grant NNX14AR62A as part of the Biodiversity and Ecological Forecasting program. Special thanks go to field assistants Dana Morton, Jeff Barr, Bob Lansdorp, Fernanda Henderikx Frietas, Christie Yorke, Justin Windsor, Selena Bowman, and future scientist Spud Simpson for allowing his parents, Miriam and Danny Simpson, to collect kelp blades in La Jolla. Conversations with Richard Zimmerman and Emanuele Di Lorenzo were helpful to the development of this paper. We would also like to acknowledge Clint Nelson, Sharron Harrer, and the many SBC LTER students for their tireless work in the Santa Barbara Channel. We would also like to thank two anonymous reviewers for their valuable comments and suggestions.

### Conflict of Interest

None declared.

Submitted 05 January 2017

Revised 27 August 2017; 24 October 2017

Accepted 25 October 2017

Associate editor: James Leichter